Simulation Analysis of Nonlinear Behavior of Pile-Soil System Based on Horizontal Loading Tests

M. SHOUJI[1], H. KASHIWA[2], Y. HAYASHI[3], K. SUITA[4], T. KURATA[5] and W. INOUE[1]

[1] *Graduate Student, Dept. of Architecture and Architectural Eng., Kyoto Univ., Kyoto, Japan*
[2] *Graduate Student, Dept. of Architecture and Architectural Eng., Kyoto Univ., M. Eng., Kyoto, Japan*
[3] *Prof., Dept. of Architecture and Architectural Eng., Kyoto Univ., Dr. Eng., Kyoto, Japan*
[4] *Assoc. Prof., Dept. of Architecture and Architectural Eng., Kyoto Univ., Dr. Eng., Kyoto, Japan*
[5] *Nippon Steel Engineering, M. Eng., Tokyo, Japan*
Email: is2.shouji@archi.kyoto-u.ac.jp

ABSTRACT :

This paper investigates the behavior of the soil around horizontally cyclic loaded pile by loading tests and the simulation analysis. Horizontal loading tests were conducted to observe the behavior of the soil under the ground through a transparent earth tank. In addition, a series of tests by using long piles were conducted to investigate effects of the ratio of the pile diameter to the pile embedment depth on nonlinear behavior of pile-soil structure. Furthermore, simulation analyses of the tests were conducted to obtain better understanding of the test results. The major findings obtained from tests and analyses are summarized as follows;
1) In case of short pile, a slip occurred in the soil around pile ends under small amplitude and at almost the same time, pile head load decreased. The slip extended to the ground surface with increasing displacement. Finally, the ground was deformed like a bump on the ground surface and pile head load became constant.
2) The test results are precisely simulated by 3-D finite element analyses. Plastic strain distribution in the soil of short pile was different from that of long pile. In case of short pile, plastic strain was concentrated in the soil around pile ends under small amplitude. With increasing displacement, the plastificated portion of the soil extended to the ground surface. The extension of the slip observed in the tests is properly simulated as the extension of the plastificated portion of the soil element.

KEYWORDS: Large displacement, Cyclic loading test, Dry sand, Pile head load, Behavior of the soil under the ground, Finite element method

1. INTRODUCTION

Since nonlinear soil-structure interaction effects under strong ground motions should be considered in the seismic design, much attention has been paid to lateral resistance of pile groups in previous researches. For instance, lateral loading tests of pile group in sand by Brown et al. (1988), horizontal loading tests to investigate the characteristics of subgrade reaction of pile group by Suzuki et al. (2003). These tests have been conducted by loading until small displacement. The test by loading until large displacement is important to investigate the effect of nonlinear soil-structure interaction on lateral resistance of pile groups. Therefore, in this study, horizontal loading tests were conducted until large displacement amplitude beyond the pile diameter.

In our previous tests, the ground was deformed like a bump on the ground surface under large amplitude. A test to observe the behavior of the soil under the ground is important to investigate the process of deforming like a bump. Such a test to observe the behavior of the soil under the ground has been conducted, for instance, the test using the X-ray picture by Kishida et al. (1985). The test by Kishida et al. has been focused on the behavior of the soil only around a pile. Therefore, our tests were conducted by using a transparent earth tank to observe the behavior of the whole soil under the ground.

On the other hand, effects of the ratio of the pile diameter to the pile embedment depth on nonlinear behavior of pile-soil structure have been reported by Tominaga et al. (1992). Therefore, a series of tests by using long piles are conducted to investigate those effects.

In addition, elastic-plastic 3-D finite element analyses of the tests were conducted to obtain better understanding of the test results. In the analyses, the pile and the soil were assumed to have plastic characteristic and the contact boundary condition was considered between the pile and the soil.

2. TEST SETUP

Tests were conducted using two kinds of earth tanks. As shown in Figure 1(a), a rigid earth tank had 3.0m length, 1.2m width, and 1.0m height. As shown in Figure 1(b), considering symmetric condition with respect to a loading direction, the width of a transparent earth tank was approximately half the size of that of the rigid earth tank, and an acrylic plate was used at one side. Grid lines consisting of color sand were placed along the acrylic plate for observation of the behavior of the soil under the ground. Piles were set in sand to a depth of 830mm for 4P and 4P-S, 580mm for 4P-T. The piles were laterally loaded at 170mm from the ground surface. The test apparatus was designed to load the piles at the caps by a rigid loading frame. The pile caps were fixed to the loading frame by high strength bolts and the pile ends were free. The loading frame was supported by guide rollers to move linearly in only one direction by a hydraulic actuator. The tests were conducted with gradually increasing displacement amplitude and the target amplitude δ normalized by the pile diameter B were 0.017B, 0.033B, 0.067B, 0.1B, 0.13B, 0.17B, 0.2B, 0.25B, 0.3B, 0.4B, 0.5B, 0.75B, and 1.0B. In each amplitude, loading was repeated for two cycles. In addition, specimens are further loaded to extremely large displacement amplitude, specifically, 2.0B and 3.0B and the number of cycle was one.

Figure 2 shows the details of the instrumentation. The piles were instrumented with strain gauges. Bending moments and shear force were estimated by the bending component of axial strain measured by the strain gauges. The total lateral load at the top of piles was measured by a load cell attached to the hydraulic actuator.

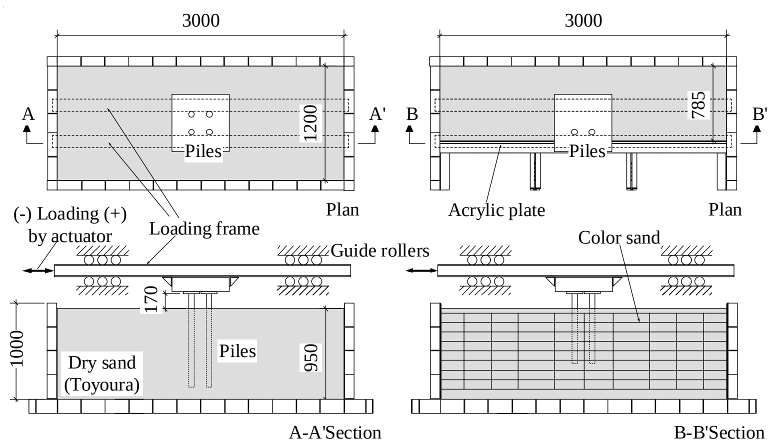

(a) Rigid earth tank (b) Transparent earth tank

Figure 1. Setup of loading tests (unit : mm)

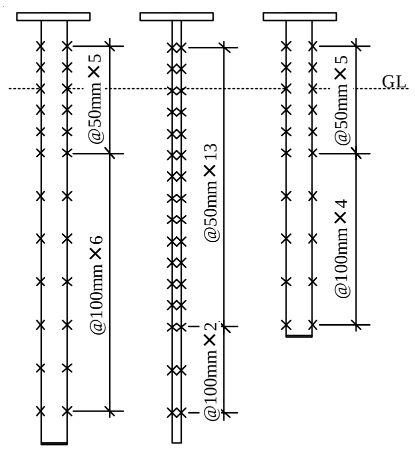

(a) 4P (b) 4P-S (c) 4P-T

Figure 2. Pile specimen and location of strain gauges

As shown in Table 1, three model tests were conducted. The test case named as 4P represented the simulation of a pile group. In the test case named as 4P-S, the pile diameter was reduced to 21.7mm without changing 2-by-2 arrangement. In the test case named as 4P-T, the number of pile was turned into 2 by using the transparent earth tank considering symmetric condition with respect to the loading direction, and the pile length was shortened to 750mm in order to avoid the plastification at the pile head. In all cases, the pile spacing was 3.0B. Dimensions and material properties of the model piles are shown in Table 2. The model piles were made of steel (STK400). The model piles for 4P and 4P-T had 60.5mm outer diameter and 8mm thickness, and the model piles for 4P-S had 21.7mm outer diameter and 1.9mm thickness.

By 'Recommendations for Design of Building Foundations', piles are classified into two groups as lateral deflections, one is the infinitely long member and the other is the infinitely short member. 'Recommendations for Design of Building Foundations' suggests the following expression for the infinitely long member:

$$\beta L > 2.25 \tag{1}$$

where $\beta=\{k_h \cdot B/(4K)\}^{1/4}$ (1/m), L=length of pile in ground (m), k_h=coefficient of horizontal subgrade reaction at 0.3B (kN/m^3), K=flexural rigidity of pile (kN・m^2). βL of 4P piles was 1.01, and that of 4P-S piles was 2.33, so that 4P piles were classified into the infinitely short piles, and 4P-S piles were classified into the long piles. In addition, 4P-T piles were also classified into the infinitely short piles because the length of 4P-T piles was shorter than that of 4P piles.

The model soil was consisted of Toyoura sand. The specific gravity, the maximum void ratio, and the minimum void ratio of Toyoura sand are 2.65, 0.95, and 0.58, respectively. The procedure to prepare the model soil was summarized as follows; 1) The soil was segmented into 10 layers and each layer was put in the earth tank softly by using a container bag carried by a crane. The soil was consisted of nine layers of 100mm depth and one layer of 50mm depth. 2) The surface of each layer was smoothed by using a trowel and compacted by using a vibrator. 3) The depth of each layer was verified by the distance from the top of the earth tank to the surface to control the relative density of each layer.

Table 1. Test case

Test name	4P	4P-S	4P-T
Number of pile	4	4	2
Relative density (%)	61	63	61
Earth tank	Rigid	Rigid	Transparent
Plan loading direction	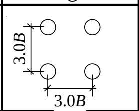	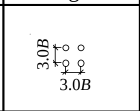	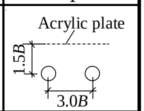
Section	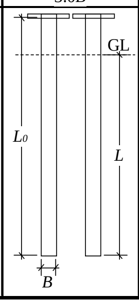	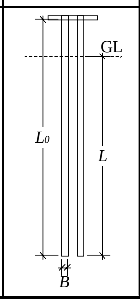	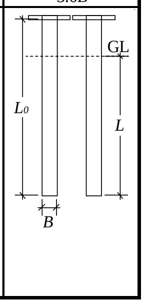

Table 2. Dimensions and material properties of the piles

Test name	4P	4P-S	4P-T
Length L_0 (mm)	1000	1000	750
Depth of embedment L (mm)	830	830	580
Outer diameter B (mm)	60.5	21.7	60.5
Thickness t (mm)	8.0	1.9	8.0
Yield stress σ_y (N/mm^2)	295	373	295
Yield moment M_y (kN・m)	4.54	0.20	4.54
Full plastic moment M_p (kN・m)	6.56	0.27	6.56

3. TEST RESULT

3.1. Ground Deformation on the Ground Surface

Plan and section views of the ground deformation for 4P, 4P-S, and 4P-T are shown in Figure 3.The solid lines show the shape of the surface of the ground around the pile groups, and the broken lines are the traces of the ground slip. In all cases, the ground outside the pile group was deformed like corn shaped hollows [refer to Figure 4(a)]. The process of this deforming was as follows; 1) The sand behind the pile moved down to the pile shaft as the pile moved, and then the ground behind the pile was deformed like a corn shaped hollow. 2) As the pile was loaded repeatedly, the corn shaped hollow was formed in both loading direction. No gap between the sand and the pile was observed. The diameter and the depth of the hollows got larger with increasing displacement amplitude.

Photographs of the ground deformation for 4P are shown in Figure 4. When the amplitude reached 0.3B, slip lines were found on the ground surface between the leading pile and the trailing pile. This slip lines were due to the gap between the ground in front of the trailing pile and the ground around the trailing pile. The ground inside the slip lines moved together with the piles. When the amplitude reached 2.0B, the ground outside the hollows was deformed like a bump on the ground surface. Similar ground deformation was observed in 4P-T, but not observed in 4P-S.

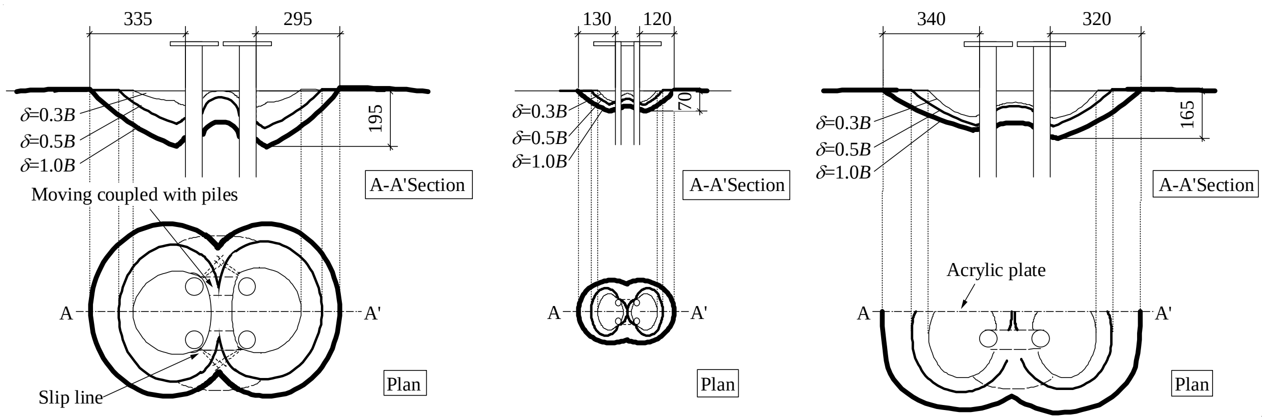

(a) 4P (b) 4P-S (c) 4P-T

Figure 3. Plan and section views of the ground deformation

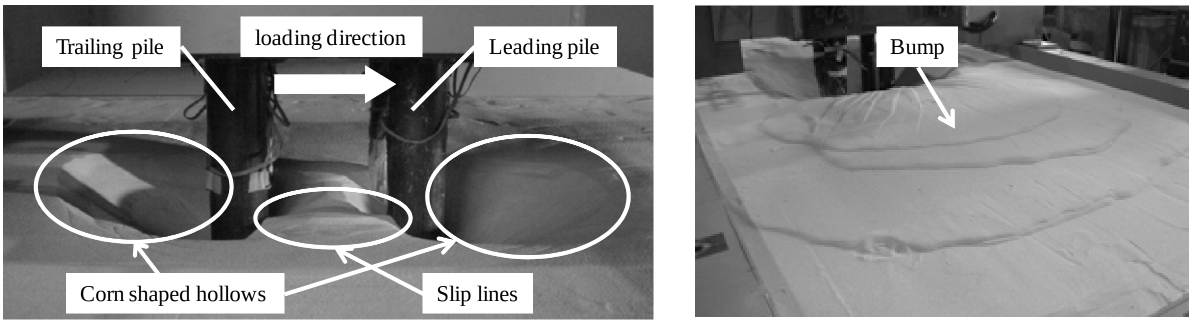

(a) Around the pile group (δ=0.3B) (b) Outside the hollows (δ=2.0B)

Figure 4. Ground deformation (4P)

3.2. Behavior of the Soil under the Ground

Behavior of the soil observed through the acrylic plate in 4P-T is shown in Figure 5. When the amplitude reached 0.3B, a slip was initiated in the soil around pile ends. This slip extended to the ground surface with increasing displacement. Finally, the ground was deformed like a bump on the ground surface.

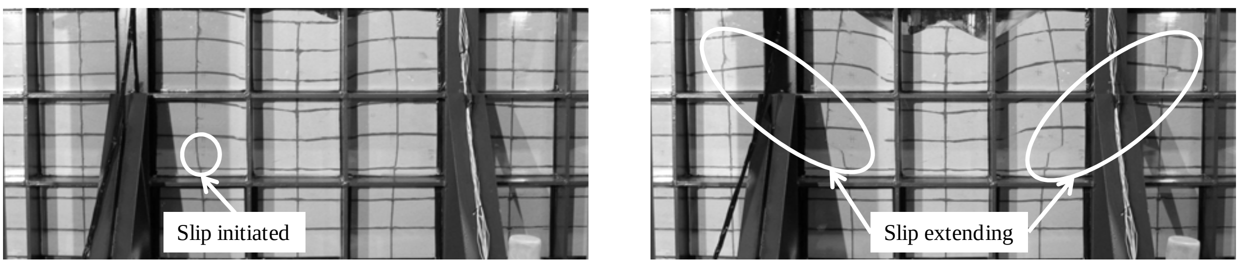

(a) δ=0.3B (b) δ=0.75B

Figure 5. Behavior of the soil on the acrylic plate

3.3. Stresses in Piles

Average load per pile - displacement relationships are shown in Figure 6. Average load per pile represents the applied load divided by the number of piles. In all cases, the hysteresis curves under cyclic loadings showed about the same shape, and the area enclosed by the curve increased with increasing displacement. In case of

4P-T, when the amplitude reached 0.5*B*, the slip in the soil extended a little and average load per pile decreased. When the amplitude reached 1.0*B*, the ground was deformed like a bump on the ground surface and average load per pile became constant. Similarly, average load per pile decreased and became constant in case of 4P, but not in case of 4P-S. For this reason, it is assumed that the slip in the soil occurred in case of 4P and 4P-T, but the slip did not occurr in case of 4P-S.

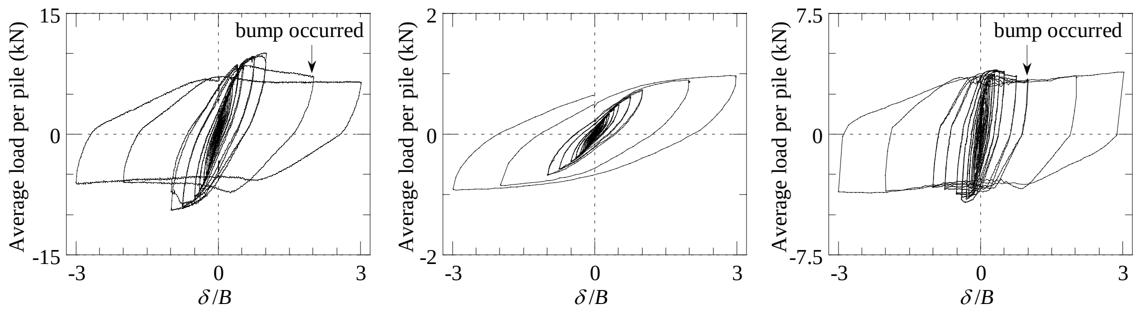

(a) 4P (b) 4P-S (c) 4P-T

Figure 6. Average load per pile - displacement relationships

4. SIMULATION ANALYSIS OF THE TESTS

4.1. Description of Model

Figure 7 shows the finite element mesh of 4P for numerical analysis. The size of the model was same as that of the test apparatus. The sides and bottom of the model of soil were fixed in all three coordinate directions with the exception of the symmetric boundary, which was only supported in the direction perpendicular to the symmetry plane. The contact condition, which allowed the slip and the separation of the contacting surfaces, was applied between the pile and the soil. The pile caps were fixed in all rotated coordinate directions and were subjected monotonic displacement in one direction. The edges of piles were free. The analyses were controlled by the horizontal displacement of the pile cap.

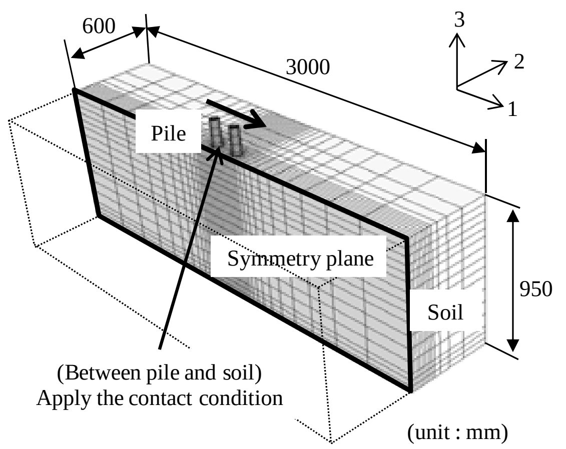

Figure 7. Layout of 3-D meshes for FEM (4P)

Table 3. Material properties used in the analyses

Pile	Yield stress σ_y (N/mm^2)	295, 370
	Coefficient of strain hardening e_t	0.01
Soil	Young's modulus E_s (N/mm^2)	4.19
	Unit weight γ (kN/m^3)	14.9
	Poisson's ratio υ	0.4
	Coefficient of earth pressure at rest K_0	0.5
	Yield Condition	Mohr-Coulomb
	Flow rule	No associated flow
	Cohesion c (N/mm^2)	0.0008
	Internal friction angle ϕ (°)	40
	Dilation Angle ψ (°)	10
Pile-Soil	Tangent friction coefficient f	0.5

The material properties used in the analyses are summarized in Table 3. The pile was assumed to be an elastic-plastic constitutive model with coefficient of strain hardening e_t and yield stress σ_y which was obtained from the uniaxial compression material testing. The soil was assumed to be a Mohr-Coulomb elastic-plastic constitutive model with no associated flow rule. The values of material properties of the soil in the analyses were determined from the previous researches which conducted similar analyses, because it was difficult to directly measure the value of material properties of the soil. The Young's modulus E_s of the soil was the average value from the ground surface to the depth of the pile end to be given by the following equation by Wakai et al (1999):

$$E_s = E_{50} = E_0 \ (p/p_0)^{0.5} \tag{2}$$

Where E_{50}=the secant elastic modulus (kN/m^2), E_0=19.6 (MPa), p_0=98 (kPa), p=the mean effective normal stress (kPa). The soil was assumed to have very small cohesion to improve the convergence of the analyses. The friction angle ϕ of the soil was 40 degree (e.g., Tatsuoka et al, 1986). The dilation angle ψ was assumed to be given by $\psi = \phi$-30 (e.g., Tatsuoka, 1993).

4.2. Ground Deformation around Piles

The deformation of the piles and the soil of 4P and 4P-S are shown in Figure 8. The gap between the trailing pile and the ground behind the trailing pile occurred in the analyses, whereas no gap was observed in the tests. The most probable cause of the gap is that the soil had very small cohesion in the analyses. By the way, in case of 4P, the gap occurred along the whole length of the pile, whereas in case of 4P-S, the gap is limited only near the ground surface. This difference about the gap measurement was due to the pile classification, i.e. 4P piles were classified into infinitely short piles, and 4P-S piles were classified into long piles.

Distribution of plastic shear strain on the ground surface for 4P is shown in Figure 9. Shear strain was concentrated in the soil between two piles. This concentration about shear strain by the analyses can well simulate the slip lines observed in the tests. As shown in Figure 8(a), almost no gap occurred behind the leading pile. As shown in Figure 9, shear strain of the ground was significantly concentrated in the soil around the trailing pile. These results indicate that the trailing pile pushed forward the ground in front of the pile, and then a gap occurred between the ground in front of the trailing pile and the ground around the trailing pile.

Distribution of plastic strain increment on the ground surface for 4P-T is shown in Figure 10. Plastic strain was concentrated in the soil in front of the leading pile. This concentration about plastic strain by the analyses can well simulate the ground deformation like a bump observed in the tests.

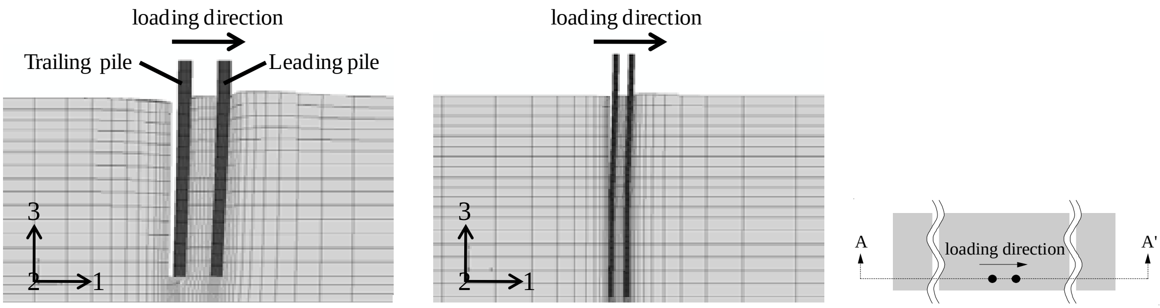

(a) 4P (b) 4P-S

Figure 8. Deformation of meshes (A-A' section, δ=0.3B)

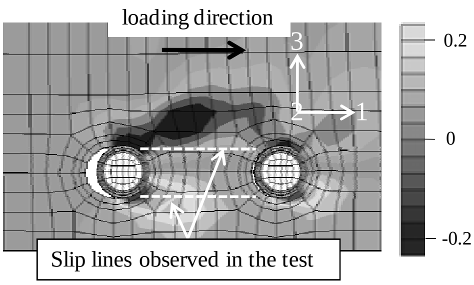

Figure 9. Distribution of plastic shear strain (4P, δ=0.3B)

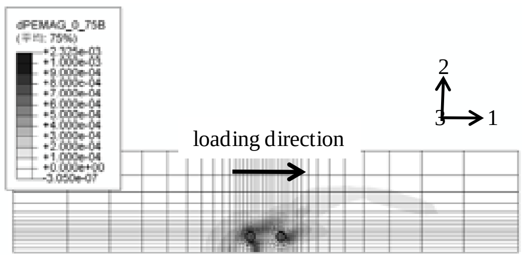

Figure 10. Distribution of plastic strain increment (4P-T, δ=0.75B)

4.3. Stresses in Piles

Bending moment distribution along each pile for 4P, 4P-S and 4P-T are shown in Figure 11. In all cases, the bending moment distribution by the analyses agree well with the aspect of test results. Shear force at each pile head for 4P-S and 4P-T are shown in Figure 12. In both cases, the shear force at each pile head by the analyses give good agreement with the test results, except that in the test result of 4P-T, the shear force of the leading pile head decreased when the amplitude reached 0.5*B* and the shear force of the trailing pile head decreased when the amplitude reached 0.4*B*.

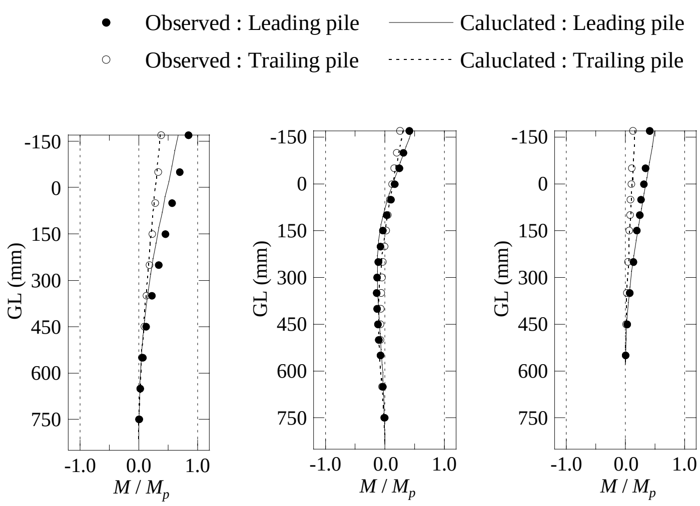

(a) 4P (b) 4P-S (c) 4P-T

Figure 11. Bending moment distributions along each pile

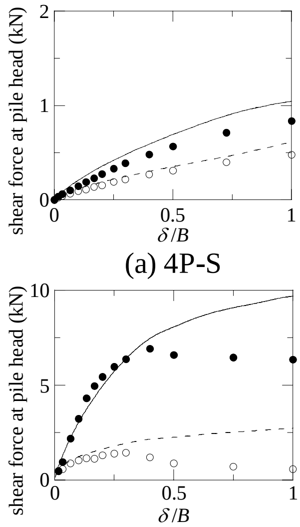

(b) 4P-T

Figure 12. Shear force at each pile head

4.4. Behavior of the Soil under the Ground

Distribution of equivalent plastic strain increment for 4P-T are shown in Figure 13. Plastic strain was concentrated in the soil around pile ends under small amplitude. With increasing displacement, the plastificated portion of the soil extended to the ground surface. This extension of the plastificated portion can be regarded as the extension of the slip observed in the tests.

Distribution of equivalent plastic strain increment for 4P-S is shown in Figure 14. Plastic strain distribution of 4P-S was different from that of 4P-T [refer to Figure 13(c)]. This difference about plastic strain distribution was due to the pile classification, i.e. 4P piles were classified into infinitely short piles, and 4P-S piles were classified into long piles.

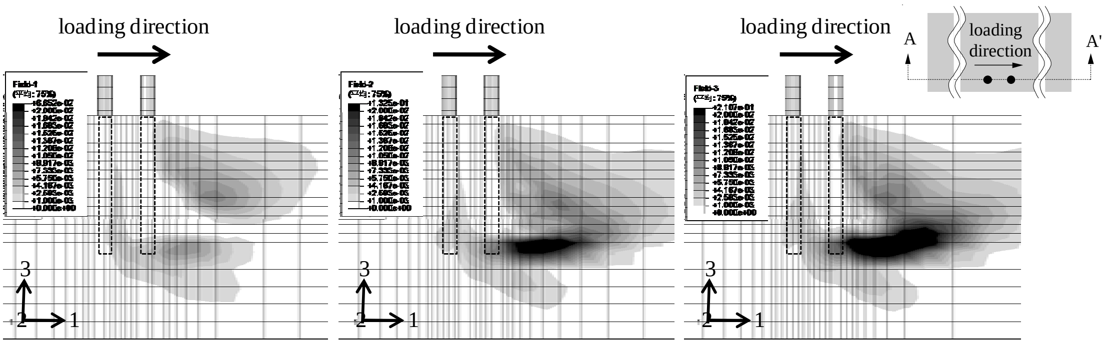

(a) δ=0.3*B* (b) δ=0.5*B* (c) δ=0.75*B*

Figure 13. Distribution of equivalent plastic strain increment (4P-T, A-A' section)

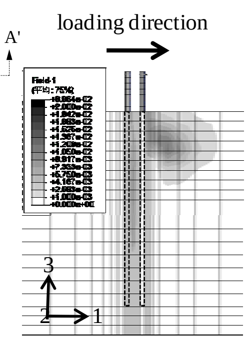

(δ=0.75*B*)

Figure 14. Distribution of equivalent plastic strain increment (4P-S, A-A' section)

5. CONCLUSION

Cyclic loading tests were conducted to observe the behavior of the soil under the ground through a transparent earth tank. In addition, a series of tests by using long piles were conducted to investigate effects of the ratio of the pile diameter to the pile embedment depth on nonlinear behavior of pile-soil structure. Furthermore, elastic-plastic 3-D finite element analyses of the tests were conducted. In the analyses, the pile and the soil were assumed to have plastic characteristic and the contact boundary condition was considered between the pile and the soil. The major findings obtained from the tests and the analyses are summarized as follows;
1) In case of short pile, a slip occurred in the soil around pile ends under small amplitude and at almost the same time, pile head load decreased. The slip extended to the ground surface with increasing displacement. Finally, the ground was deformed like a bump on the ground surface and pile head load became constant.
2) The test results, such as ground deformations and stresses in piles, are precisely simulated by 3-D finite element analyses. Plastic strain distribution in the soil of short pile was different from that of long pile. In case of short pile, plastic strain was concentrated in the soil around pile ends under small amplitude. With increasing displacement, the plastificated portion of the soil extended to the ground surface. This extension of the plastificated portion is regarded as simulating the extension of the slip observed in the tests.

Thus, the validity of the presented analysis model for simulating non-linear behavior of pile-soil structure including large deformation range is confirmed.

REFERENCES

AIJ. (2001). Recommendations for Design of Building Foundations, AIJ, Tokyo, Japan

Brown, D. A., Morrison, C., Reese, L. C. (1988). Lateral Load Behavior of Pile Group in Sand. *Journal of Geotechnical Engineering*, ASCE, **114:11**, 1261-1276.

Kashiwa, H., Kurata, T., Hayashi, Y., Tamura, S., Suita, K. (2007). Displacement amplitude dependence of effect of pile group by cyclic lateral loading tests on large displacement. *Journal of Structural and Construction Engineering Architectural Institute of Japan* **614**, 53-60. (in Japanese)

Kishida, K., Suzuki, Y., Nakai, S. (1985). Behavior of a pile under horizontal cyclic loading. *Proceedings of the Eleventh International Conference on Soil Mechanics and Foundation Engineering* **4**, 1413-1416.

Kurata, T., Kashiwa, H., Hayashi, Y., Tamura, S., Suita, K. (2007). Non-linear behavior of pile group-soil system based on horizontal loading test subjected to large displacement. *Journal of Structural and Construction Engineering Architectural Institute of Japan* **614**, 45-52. (in Japanese)

Suzuki, Y., Adachi, N. (2003). Relation between subgrade reaction and displacement of model pile group based on horizontal loading test. *Journal of Structural and Construction Engineering, the Architectural Institute Japan* **570**, 115-122. (in Japanese)

Tatsuoka, F. (1993). Introduction to Strength of Soil and Failure of Ground (Third Revision), The Japanese Geotechnical Society. (in Japanese)

Tominaga, K., Yamamoto, H., Yamashita, H. (1992). Experimental study of effect of embedded length on behavior of laterally loaded piles. *Journal of Structural and Construction Engineering, the Architectural Institute Japan* **438**, 127-136. (in Japanese)

Wakai, A., Gose, S., Ugai, K. (1999). 3-D elasto-plastic finite element analyses of pile foundations subjected to lateral loading. *Soil and foundations* **39:1**, 97-111.